Systematic measurements of dose-dependent responses for combinatorial treatments of SA and JA led to the development of transcriptomic biomarkers

Atsuki Tomita[1,2], Taro Maeda[1], Natsumi Mori-Moriyama[3], Yasuyuki Nomura[3], Yuko Kurita[4], Makoto Kashima[5], Shigeyuki Betsuyaku[6], Atsushi J. Nagano[1, 7*]

[1] Institute for Advanced Biosciences, Keio University, Tsuruoka, Yamagata 997-0052, Japan

[2] Graduate School of Media and Governance, Keio University, Fujisawa, Kanagawa 252-0882, Japan

[3] Research Institute for Food and Agriculture, Ryukoku University, Otsu, Shiga 520-2194, Japan

[4] Graduate School of Life Sciences, University of Tokyo, Bunkyo-ku, Tokyo 113-8657, Japan

[5] Faculty of Science, Toho University, Funabashi, Chiba, 274-8510, Japan

[6] Faculty of Agriculture, Ryukoku University, Otsu, Shiga 520-2194, Japan

[7] Bioscience and Biotechnology Center, Nagoya University, Nagoya, Aichi, 464-8601, Japan

Corresponding Author:

Atsushi J. Nagano

Bioscience and Biotechnology Center, Nagoya University, Nagoya, Aichi, 464-8601, Japan

Email: anagano@agr.nagoya-u.ac.jp

ABSTRACT

Salicylic acid (SA) and jasmonic acid (JA) regulate plant defense against pathogens and herbivores. The SA-JA pathways often interact antagonistically with the induction of one, leading to the suppression of the other. However, the effect of combined SA/JA concentrations on plant responses is unknown. Here, we show transcriptional responses specific to combinations of SA and JA concentrations and develop transcriptomic biomarkers to estimate SA/JA response states. Combinatorial treatments with eight concentrations of SA and JA, combined with large-scale transcriptome analysis, revealed 43 different expression patterns, including not only well-known antagonistic responses but also responses specific to combinations of SA/JA concentrations. Notably, the expression of *CYP94B3*, a key enzyme involved in JA-Ile turnover, was finely tuned by specific SA/JA concentration combinations being induced under high SA conditions in a JA dose-dependent manner. In addition, the expression peaks of indole glucosinolate biosynthesis genes were found at approximately 30-fold higher JA concentrations than aliphatic glucosinolate biosynthesis genes. Furthermore, to quantitatively estimate SA/JA response states, we developed transcriptomic biomarkers using a machine learning approach. The marker specifically estimated response states to target phytohormones. Through analysis of *npr3/4* double mutants, we confirmed that the biomarkers were applicable to the analysis of mutants. The biomarkers will allow us to extract insights into phytohormone responses from various large-scale transcriptome data, e.g., field transcriptomics and single-cell RNA-Seq.

(219 / 250 words)

Keywords: Salicylic acid, Jasmonic acid, transcriptome, biomarker

Running head: Transcriptome analysis of response to SA/JA concentration in *A.thaliana*

INTRODUCTION

When plants suffer environmental stresses, they produce various phytohormones that regulate resistance mechanisms. The plants respond to a wide range of biotic stresses through the production of salicylic acid (SA) and jasmonic acid (JA). Salicylic acid (SA) is a phytohormones required for plant defense against pathogens (Maruri-López et al., 2019). Pathogen infection induces biosynthesis of SA in infected tissues (Mishina and Zeier, 2007). SA-responsive genes include pathogenesis-related (PR) proteins that have antimicrobial properties (Jain and Khurana, 2018). Phytohormone regulate various physiological processes in plants at nanomolar concentrations (Munné-Bosch and Müller, 2013). SA response is an example of a response altered by quantitative concentrations. When intracellular SA levels are high, the SA receptors, NPR3 and NPR4, induce programmed cell death that prevents the establishment of parasitism(Dodds and Rathjen, 2010; Fu et al., 2012). Jasmonic acid (JA) is a phytohormones synthesized against insects and necrotrophic pathogens (Ghorbel et al., 2021; Wasternack and Hause, 2013). The JA pathway, induced by signals from insect saliva and damaged cells, promotes widespread insect resistance (Howe and Jander, 2008). JA induces glucosinolate (GSL) biosynthesis (Fritz et al., 2010; Guo et al., 2013). In Brassicaceae, GSLs are chemical defense substances that act directly against insects and microbes (Hopkins et al., 2009; Wittstock and Burow, 2010). It is known that different types of GSLs are induced depending on the type and timing of external threats (Abuyusuf et al., 2023).

The crosstalk between salicylic acid (SA) and jasmonic acid (JA) signaling pathways in plant defense is characterized by reciprocal antagonism (Hou and Tsuda, 2022; Thaler et al., 2012). This antagonism is likely adaptive, allowing plants to fine-tune their defense responses against different types of attackers (Pieterse et al., 2001; Pieterse and Dicke, 2007). In *Arabidopsis*, the regulatory protein NPR1 mediates the crosstalk by facilitating SA-induced suppression of JA signaling through its cytosolic function (Spoel et al., 2003). The antagonistic interaction between SA and JA pathways can modulate the expression of defense genes and

74 affect gene-for-gene resistance to pathogens. The JA-insensitive *coi1* mutation restored
75 CMV(Y)-activated expression of SA-dependent PR genes in an SA-deficient background,
76 demonstrating the complex interplay between these pathways(Takahashi et al., 2004). The
77 interaction between SA and JA is generally antagonistic, but there are some exceptions. During
78 effector-triggered immunity, simultaneous accumulation of SA and JA was observed,
79 necessitating the activation of both signaling pathways (Kenton et al., 1999; Liu et al., 2016;
80 Tsuda et al., 2009). Interaction of SA and JA signaling pathways can also result in synergistic
81 defense and oxidative stress effects leading to cell death (Mur et al., 2006; Zhang et al., 2020).
82 Furthermore, simultaneous activation of SA-dependent systemic acquired resistance and JA-
83 dependent induced systemic resistance has been shown to have additive effects on induced
84 defense against pathogens (Niu et al., 2011; Van Wees et al., 2000). Cooperative interactions
85 between SA and JA have been frequently observed. However, their detailed mechanisms remain
86 unclear. SA and JA signaling levels are controlled by the plant itself and manipulated by external
87 enemies (Spoel et al., 2007). For example, *Pseudomonas syringae* promotes pathogenicity by
88 producing coronatine that mimic jasmonic acid isoleucine (Zheng et al., 2012). Herbivores also
89 manipulate SA and JA signaling levels using salivary enzymes to weaken plant wounding
90 responses (Weech et al., 2008). It is suggested that SA and JA signaling levels are altered by
91 both the plant's own responses and external enemies' manipulation. To fully understand the
92 complex interplay of SA/JA signaling pathways, it is important to analyze the plant's response
93 to a range of SA and JA concentrations and their combinations.

94 Systematic transcriptome analysis using the various combinations of SA and JA
95 concentrations is essential for a comprehensive understanding of SA-JA crosstalk (Robert-
96 Seilaniantz et al., 2011). Although, there are several small-scale studies that have measured the
97 dose response of SA and JA (Hickman et al., 2019; Mur et al., 2006; Zhang et al., 2020), most
98 previous studies on SA-JA crosstalk have been comparisons between with and without
99 treatment. Because massive RNA-Seq experiments are required, it is challenging to

100 systematically analyze the various combinations of SA and JA concentrations. On the other
101 hand, various high-throughput RNA-Seq library preparation methods have been proposed
102 (Bjornson et al., 2020; Kamitani et al., 2019; Kashima et al., 2020; Santacruz et al., 2022).
103 Using such technical advances, large-scale transcriptome projects emerged in recent years. For
104 example, effects of temperature, daylength and circadian clock were systematically analyzed
105 using rice seedlings (Hashida et al., 2024). The data enhanced the model to predict
106 transcriptome dynamics under complex field conditions.

107 In this study, we systematically analyzed plant responses to combinations of various
108 SA/JA concentrations and developed a transcriptomic biomarker for SA/JA. We treated *A.*
109 *thaliana* seedlings with 64 combinations of SA and JA concentration and quantified
110 transcriptomes using high-throughput RNA-seq (Kamitani et al., 2019; Kashima et al., 2020).
111 The systematic data enable us not only to revealed the diverse responses of genes to SA/JA
112 concentrations but also to create a transcriptomic biomarker that specifically estimates SA/JA
113 response states.
114
115
116

117

118 **RESULTS**

119 *Expression topography of SA/JA responses revealed by high-throughput RNA-seq*

120 In order to evaluated how SA/JA concentration affects the interaction between the SA
121 and JA signaling pathways, we performed transcriptome profiling of *A. thaliana* seedlings
122 treated for 6 hours to 64 different SA/JA concentrations combinations (Fig. 1A, B,
123 Supplementary Table S1). We employed an assay system that allows the simultaneous
124 processing of 96 samples using 96-well plates (Fig. 1A, B). We used at least four biological
125 replicates per a treatment condition for RNA-seq. In total, 384 samples were processed. 370
126 samples with more than $10^{5.5}$ reads were used for further analysis (Supplementary Fig. S1A, B).
127 The 12,963 genes with an average expression level higher than 1.5 on the log2(RPM+1) scale
128 were designated as expressed genes and used for further analysis (Supplementary Fig. S1A, C).
129 In this study, a gene expression pattern by SA/JA concentration was called an expression
130 topography (Fig. 1C-F).

131 We evaluated the expression topography of well-known marker genes involved in the
132 SA/JA response, as well as two genes associated with JA metabolism. The marker gene for the
133 SA response, *PR1*, exhibited an expression threshold at 0.033 mM SA. When JA was treated
134 with 1 mM, the expression of *PR1* was completely suppressed. The optimal concentration of
135 SA for *PR1* expression was 0.33 mM (Fig. 1C, Supplementary Fig. S2A). The marker gene for
136 the JA response, *VSP1*, exhibited an expression threshold at 0.001 mM JA. The optimum
137 concentration of JA for *VSP1* expression was 0.1 mM (Fig. 1D, Supplementary Fig. S2B).
138 These results are consistent with the qualitative understandings of SA/JA responses and SA and
139 JA antagonism in previous studies (Hou and Tsuda, 2022; Mur et al., 2006; Spoel et al., 2003;
140 Thaler et al., 2012). Figure 1E shows the expression of *LOX3*, which was increased under 0mM
141 to 0.33mM JA conditions in a JA concentration-dependent manner. *LOX3* encodes the enzyme

142 for the first step of JA synthesis (Chauvin et al., 2016). JA biosynthesis in plants exhibits a
143 positive feedback loop with the pathway including key enzymes such as *LOXs* upregulated
144 dose-dependently by JA (Yang et al., 2020). The increase of *LOX3* expression in response to
145 JA concentrations ranging from 0 to 0.33 mM is consistent with previous studies showing a
146 positive feedback loop in JA biosynthesis. Interestingly, *LOX3* expression was suppressed
147 under 1 mM SA/JA treatment, suggesting that the positive feedback loop of *LOX3* is terminated
148 once JA/SA levels reach substantial accumulation (Fig. 1. E, Supplementary Fig. S2C). In
149 contrast, the expression of *CYP94B3*, a key regulator in the suppression of the JA signaling
150 cascade, decreased in a JA concentration-dependent manner (Fig. 1F, Supplementary Fig. S2D).
151 CYP94B3 oxidizes the bioactive form of JA, jasmonoyl-L-isoleucine (JA-Ile). This oxidation
152 by CYP94B3 regulates JA signaling levels and could affect SA/JA crosstalk (Kitaoka et al.,
153 2014; Koo et al., 2011). Interestingly, *CYP94B3* expression was most upregulated under high
154 SA conditions, showing a 4.6-folds increase between 0 mM and 1 mM SA in the presence of 1
155 mM JA.

156 To visualize transcriptome-wide characteristics in response to SA and JA treatments,
157 we conducted a principal component analysis (PCA) and detection of differentially expressed
158 genes (DEGs). The PCA was performed on 370 samples with expressed genes. The principal
159 component 1 explained 19.3% of variance and coordinated with the SA treatment
160 concentrations (Fig. 1G, Supplementary Fig. S3A). The principal component 2 explained 6.7%
161 of variance and coordinated with the JA treatment concentrations (Fig. 1H, Supplementary Fig.
162 S3B). No apparent differences were observed among the 96 well plates (Fig. 1I, Supplementary
163 Fig. S3C-F). The number of DEGs between control and phytohormone-treated samples
164 increased in a dose-dependent manner for SA and JA (Supplementary Fig. S4A-C). For both
165 SA and JA, there was a larger number of up-regulated genes than down-regulated genes in most
166 conditions from the 0 mM to 0.33 mM treatments (Supplementary Fig. S4D). In contrast, the

167 number of down-regulated genes exceeded that of up-regulated in the 1 mM treatment.

168

169 *Expression topography revealed diverse responses of genes to SA/JA concentrations*

170 3,001 genes whose expression varied with the treatment of SA/JA were selected as
171 SA/JA responsive genes (Supplementary Fig. S1A, D) and used for the following analysis. Each
172 SA/JA responsive gene was normalized by Z-scoring and smoothed by a 3x3 moving average
173 filter to extract key characteristics of the expression topography. We performed clustering of
174 the SA/JA responsive genes by affinity propagation. The affinity propagation determined 43
175 clusters based on the expression topography (Fig. 2A). The clusters contained 23 − 299 genes.
176 We found that genes with a similar pattern were enriched in clusters (Fig. 2B). Gene expression
177 of cluster A-02 increased in a concentration-dependent manner in response to JA and decreased
178 in a concentration-dependent manner in response to SA. On the other hand, gene expression of
179 cluster C-01 increased in a concentration-dependent manner in response to SA and decreased
180 in a concentration-dependent manner in response to JA. To classify the clusters to groups,
181 hierarchical clustering was performed using Pearson's correlation coefficients among
182 expression topographies of the clusters. The optimal number of groups was estimated, and the
183 clusters were classified into group A to H (Fig. 2C). Group F was the largest group and had
184 1,435 genes, which was about half of the 3,001 SA/JA-affected genes. In contrast, the smallest
185 group was the group G containing 74 genes (Fig. 2A). Group B had an expression topography
186 that was up-regulated by high concentrations of SA and JA. By contrast, group F had an
187 expression topography that was down-regulated by high concentrations of SA and JA. The
188 expression of group D was enhanced at intermediate concentrations of SA and was not reduced
189 by increasing JA concentrations.

190

191 *Expression topographies are associated with gene functions*

192 To examine whether genes with similar expression topographies shared biological
193 functions, enrichment analysis was conducted on 43 clusters. Eighteen clusters were found to
194 be enriched with 1-103 GO terms (adjusted $P < 0.05$, Fig. 3A, Supplementary Table. S2). Genes
195 in cluster A-02 were enriched in GO terms "response to jasmonic acid" (GO:0009753, adjusted
196 $P = 4.09 \times 10^{-4}$). This cluster contained many JA-responsive genes reported in previous studies,
197 such as *VSP2*, *JAZ8*, *JAZ10* and *JOX3* (Fernández-Calvo et al., 2011). Cluster C-01 showed the
198 expression induced by SA and suppressed by JA. The *PR1* gene was contained in this cluster.
199 Multiple GO terms were enriched in cluster C-01, including "response to bacterium"
200 (GO:0009617, adjusted $P = 1.18 \times 10^{-7}$) and "response to salicylic acid" (GO:0009751, adjusted
201 $P = 3.55 \times 10^{-6}$). When both SA and JA were treated in high concentrations, genes in cluster B-
202 01 were up-regulated and genes in clusters F-07 and F-08 were down-regulated. In cluster B-
203 01, GO terms such as "protein folding" (GO:0006457, adjusted $P = 2.68 \times 10^{-5}$) and "response
204 to reactive oxygen species" (GO:0000302, adjusted $P = 1.61 \times 10^{-3}$) were enriched. The cluster
205 B-01 mainly comprised genes encoding heat shock proteins such as HSP17.4 and HSP17.6.
206 Clusters F-07 and F-08 were enriched in GO terms such as "ribosome biogenesis" (GO:
207 0042254, adjusted $P = 7.71\times 10^{-30}$ and 5.31×10^{-4}) and "translation" (GO: 0006412, adjusted P
208 $= 1.52 \times 10^{-75}$ and 3.28×10^{-2}). GO terms associated with "photosynthesis" (GO:0015979,
209 adjusted $P = 1.57 \times 10^{-4}$ and 4.22×10^{-3}) were enriched in clusters F-05 and F-06. Genes in the
210 clusters F-05 and F-06 were down-regulated in a dose-dependent and additive manner by SA/JA
211 co-treatment (Fig. 3A). These results were consistent with previous studies, which
212 demonstrated that co-treatment with SA and JA reduced the expression of photosynthesis-
213 related genes (Hickman et al., 2019; Schweiger et al., 2014; Zhang et al., 2020).
214 Based on analysis of the expression topography, we found that two subtypes of GSLs
215 were induced by different concentrations of JA. In cluster E-01, the GO term "glucosinolate
216 biosynthetic process" (GO:0019761, adjusted $P = 5.32 \text{ x } 10^{-3}$) was significantly enriched (Fig.
217 3A). Interestingly, "glucosinolate biosynthetic process" was also significantly enriched in

218 cluster F-02 (adjusted P = 8.22 x 10^{-3}). The cluster E-01 contained genes related to indole
219 glucosinolate biosynthesis, *e.g. SUR1, CYP83B1, CYP79B3, MAM*. In contrast, the cluster F-
220 02 contained genes related to aliphatic GSL biosynthesis, *e.g. MAM3, CYP79F2, BCAT4,*
221 *SOT18*. The expression peak of indole GSL biosynthesis genes was found at lower
222 concentration of JA than that of aliphatic GSL (Fig. 3B-K). In low SA concentrations (0 ~ 0.01
223 mM), the expression peaks of indole GSL biosynthesis genes were found around 0.1 mM JA
224 (Fig. 3B). On the other hand, the expression peaks of aliphatic GSL biosynthesis genes were
225 found around 0.003 mM JA (Fig. 3B). The expression peaks of indole GSL-related genes were
226 found at approximately 30-fold higher JA concentrations than that of aliphatic GSL-related
227 genes. This response was specific to low SA concentrations (Fig. 3C, Supplementary Fig. S5).
228
229 *No single gene was a specific and quantitative SA/JA response marker*
230 Our comprehensive dataset allowed us to systematically evaluate how the expression
231 of a single gene correlated with treated concentrations of SA and JA (Fig. 4A, B, C,
232 Supplementary Table. S3). *PR1* and *VSP1* have long been used as expression markers of SA
233 and JA response (Javed et al., 2025; Zhang et al., 2020). Correlation coefficients between *PR1*
234 and treatment concentrations of SA/JA were 0.63 and -0.30, respectively (Fig.4C). Correlation
235 coefficients between *VSP1* and SA/JA treatment concentrations were -0.20 and 0.07,
236 respectively (Fig.4C). *PR1* had the 29th highest correlation with SA concentration. On the other
237 hand, *VSP1* had the 4,695th highest correlation with JA concentration. The genome-wide
238 pattern of correlations indicated that correlations with SA and JA were associated with each
239 other (fig. 4C). The gene with the highest correlation with SA treatment concentration was
240 *HRG2*. The correlation with SA was 0.74 and that with JA was 0.14 (Fig. 4C, D). The gene
241 having the highest negative correlation with SA was *UL4Z*, with a correlation of -0.70 with SA
242 and - 0.22 with JA (Fig. 4C, E). The gene with the highest positive correlation with JA treatment
243 concentration was *AT2G47950*. The correlation with JA was 0.85 and that with SA was 0.16

244 (Fig. 4C, F). The gene having the highest negative correlation with JA was *SAUR6*, with a
245 correlation of -0.68 with JA and -0.44 with SA (Fig. 4C, G). These four genes respond in a
246 threshold manner to specific concentrations of SA/JA (Fig. 4D-G). These results showed
247 difficulty in identifying a gene whose expression served as a specific and quantitative response
248 marker.
249
250 *Development of a transcriptomic biomarker of SA/JA response state*
251 To overcome the limit of using a single gene as a response marker, we developed a
252 transcriptomic biomarker of the SA/JA response state. This enabled the estimation of the SA/JA
253 response state corresponding to a specific treatment concentration of SA/JA. To create a
254 transcriptomic biomarker that correlated with SA/JA and uncorrelated with their counterpart,
255 we employed the method using ensemble learning and L1-regularized linear regression,
256 LASSO (Fig. 5A). The transcriptome data of 370 samples at 64 concentration conditions were
257 used as training data. We also obtained additional transcriptome data of 101 samples at 25
258 conditions of SA and JA combining 5 concentrations: 0, 0.001, 0.01, 0.1, and 1 mM
259 (Supplementary Fig. S6). The transcriptome data were used as test data for validating predictive
260 performance of the markers. The predicted values of markers for the training data highly
261 correlated with the treated concentrations of SA/JA (0.98 for SA and 0.98 for JA, Fig. 5B, C).
262 For the test data, correlation coefficients between the predicted concentrations of the markers
263 and the treated concentrations of their target phytohormones were 0.97 for SA and 0.96 for JA
264 (Fig. 5D, E). These correlation coefficients were higher than the best correlated single genes
265 (Fig. 4). As the treated concentration increased, the predicted concentration also gradually
266 increased. However, in the high concentration range, the predicted concentrations were
267 underestimated. On the other hand, correlation coefficient between the predicted SA
268 concentrations and the treated JA concentration was -0.11 (Fig. 5F), and correlation coefficient
269 between the predicted JA concentrations and the treated SA concentration was 0.10 (Fig. 5G).

These results showed that the transcriptomic biomarkers worked in a specific and, at least relatively, quantitative manner. Our ensemble learning approach allowed us to evaluate contributions of genes to the marker. To reveal the genes contributing the marker, we calculated the selection frequency of genes in the transcriptomic biomarker (Supplementary Fig. S7). The distributions of selection frequencies indicated that limited number of genes were frequently used in the marker. The numbers of highly selected genes with a selection frequency of 0.95 or higher were 140 for JA and 95 for SA. The highly selected genes included genes known as SA/JA responsive genes. ,The highly selected genes for JA included *JAZ1*, *JAZ2*, *JAZ3*, *JAZ5*, *JAZ6*, *LOX2*, and *ATGSTU1*. The highly selected genes for SA included *ZAR 1*, *WRKY18*, *WRKY70*, *ROXY18*, *ECS1*, and *ARR4* (Supplementary Table 3).

As a use case of the transcriptomic biomarker of the SA/JA response state, we investigated the responses to SA/JA in *npr3/4* double mutants: *npr3-1npr4-3* and *npr3-2npr4-2* (Fig. 6, Supplementary Fig. S6). We obtained transcriptome data of 87 samples for *npr3-1npr4-3* and 107 samples for *npr*3-*2npr4-2* at 25 conditions of SA and JA combining 5 concentrations. By applying transcriptomic biomarker to the transcriptome data, we estimated the SA/JA response state of *npr3/4* double mutants (Fig. 6). The mutants showed significantly higher predicted SA concentration than that in Col-0 for all SA treatment conditions except 1 mM SA (Fig. 6C, D). In other words, the mutants seemed to have a higher sensitivity to SA than Col-0. These results suggested that NPR3/4 suppressed the SA signaling pathway in conditions with lower than 1mM SA. These results were consistent with previous studies showing that NPR3 and NPR4 acted as transcriptional co-repressors of SA-responsive genes (Ding et al., 2018; Fu et al., 2012). On the other hand, when we focused on responses to JA, we found significant differences between mutants and Col-0 in several conditions (Fig. 6A, B). However, the responses were not consistent among mutant alleles.

295 **DISCUSSION**

296 Our systematic analysis combining phytohormone treatments with large-scale
297 transcriptome profiling has provided novel hypotheses and insights into SA/JA concentration-
298 dependent responses. For instance, *CYP94B3* expression increased in a JA dose-dependent
299 manner and enhanced at high SA concentrations (Fig. 1D, F). The 12-OH-JA-Ile produced by
300 CYP94B3 exhibits weaker JA signaling compared to the JA-Ile (Saito et al., 2023). The
301 decreased expression of JA-responsive downstream genes, such as *VSP1* and cluster A-02,
302 coincided with the increased expression of *CYP94B3*. Attenuation of the JA pathway by
303 CYP94B3 relieves suppression of the SA pathway, consequently enhancing resistance against
304 *Pseudomonas syringae* pv. tomato DC3000 (Aubert et al., 2015; Hwang and Hwang, 2010).
305 These findings suggest that JA-Ile oxidation by CYP94B3 has a role in SA-mediated defense
306 response triggered by high SA concentrations induced during infection. Additionally, JA dose-
307 dependent expression of *CYP94B3* indicates a mechanism to prevent excessive oxidation of JA-
308 Ile. Although an SA concentration-dependent transcriptional regulation model involving
309 NPR1/NPR3/NPR4 has been proposed (Ding et al., 2018; Fu et al., 2012), the combined SA
310 and JA concentration-dependent regulation of transcription remains unclear. Further
311 investigation is required to understand the transcriptional regulatory mechanisms triggered by
312 the concentrations of SA/JA, such as *CYP94B3*.

313 We identified that combinations of SA/JA concentrations control most genes that share
314 a biological function. The peak expression of indole GSL biosynthesis-related genes was
315 detected at 30-fold higher JA concentrations than aliphatic GSL biosynthesis-related genes (Fig.
316 3B). Indole-3-carbinol and indole-3-acetonitrile, breakdown products from indole GSL,
317 primarily inhibit pathogen growth (Aires et al., 2009; Madloo et al., 2021). Feeding damage to
318 leaves provides entry points for pathogenic bacteria (Grode et al., 2017; Savatin et al., 2014).
319 High concentrations of JA accumulating around damaged cells (Glauser et al., 2009) suggests
320 the production of indole GSL to prevent secondary damage caused by pathogens. In contrast,

321 sulforaphane, a breakdown product from aliphatic GSL, negatively affects a wide variety of
322 herbivores (Jeschke et al., 2016). JA accumulation is quantitatively lower in undamaged leaves
323 compared to damaged ones (Ohnmeiss et al., 1997). Relatively low concentrations of JA likely
324 enhance the synthesis of aliphatic GSL, inhibiting subsequent insect feeding. JA concentrations
325 may be critical for inducing different types of GSLs in damaged and undamaged tissues to
326 counteract the specific natural enemies anticipated in each tissue.

327 Although in this study we quantified the response of Arabidopsis seedlings to a wide
328 range of SA/JA concentrations and combinations, the data from this study are still insufficient
329 to elucidate the entire picture of the SA/JA responses. Tissue-specific and cell-type-specific
330 responses could be overlooked because the whole seedling was used as the sample for RNA-
331 Seq. Our measurement of total RNA amounts of shoot and root indicated that approximately
332 70% of total RNA of seedling was derived from shoot and 30% from root (Supplementary Fig.
333 S8A). Responses of root-specific highly expressed genes were successfully measured
334 (Supplementary Fig. S8B). However, if a gene that is expressed in both shoot and root shows
335 opposite responses in shoot and root, the responses would be offset and undetectable. Specific
336 responses in minor cell types would also be undetectable. Combining systematic SA/JA
337 treatment with single-cell RNA-Seq analysis would help overcome these limitations. In
338 addition to such tissue-specific responses, the influence of other hormones on SA/JA responses
339 could be overlooked in our analysis. For example, abscisic acid, ethylene, brassinosteroid
340 modulates SA and JA signaling pathways (Basit et al., 2021; Gupta et al., 2024; Li et al., 2019).
341 Transcriptome profiling on combinatorial concentration treatments with other phytohormones
342 is needed to quantitatively clarify a broader phytohormone signaling network. The throughput
343 of our transcriptome profiling on combinatorial concentration treatments is enough high to
344 expand the approach of this study to interactions between multiple phytohormones.

345 The transcriptomic biomarker that we developed in this study to predict SA/JA
346 response status is expected to have a variety of applications. It is important to quantitatively

evaluate the response states for multiple phytohormones (Pan and Wang, 2009; Šimura et al., 2018). Phytohormone quantification by mass spectrometry has been intensively developed and achieved very high sensitivity and accuracy (Kojima and Sakakibara, 2012; Petřík et al., 2024). It is suggested that for some reasons, the measured phytohormone levels do not always correspond to the response states (Vrobel and Tarkowski, 2023). Possible factors contributing to this discrepancy include receptor sensitivity, interactions among hormone signaling pathways and difficulty in distinguishing biologically active hormones from inactive conjugates. Complementary use of our transcriptomic biomarkers and the hormone quantifications will help to elucidate how this discrepancy arises. The transcriptomic biomarkers could be applicable to large-scale transcriptome data in emerging research areas: single-cell transcriptomics and field transcriptomics. A study combining single-nucleus RNA-Seq and spatial transcriptomics to analyze plant immune responses has been reported recently (Nobori et al., 2025). Applying the transcriptomic biomarkers to such datasets would reveal SA/JA response dynamics during plant immune responses at a single-cell resolution. In field transcriptomics, large amounts of transcriptome data acquired in the outdoor field are modeled with meteorological data to reveal the responses of organisms in real environments (Nagano et al., 2012). Large-scale field transcriptome studies consisting of hundreds or thousands of samples over several years have been reported in recent years (Hashida et al., 2024; Kashima et al., 2021; Nagano et al., 2019). Integrating the field transcriptome studies with SA/JA transcriptomic biomarkers would facilitate a systematic analysis of the interactions among climate factors and plant defense responses.

370

371 **MATERIALS AND METHODS**

372 *Plant materials and SA/JA treatment*

373 We used *Arabidopsis thaliana* (Col-0: CS70000, *npr3-1npr4-3*: CS72351 and *npr3-*
374 *1npr4-3*: CS72352) to analyze the responses to SA & JA concentrations. The seeds of these
375 lines were obtained from the Arabidopsis Biological Resource Center. Methyl jasmonate (135-
376 14411, FUJIFILM Wako, Osaka, Japan) and sodium salicylate (S3007, Merck, Darmstadt,
377 Germany) were dissolved to 1 M in ethanol or water, respectively. 100× SA or 100× JA stock
378 solutions were then diluted from 1 M stock to 0 mM, 0.1 mM, 0.33 mM, 1 mM, 3.3 mM, 10
379 mM, 33 mM, and 100 mM in ethanol or water, respectively. Sixty-four variations of 50× SA/JA
380 mixed stock solutions were prepared by combining eight concentrations of 100× SA and 100×
381 JA, and mixing equal amounts of each. These 64 stock solutions for SA/JA treated samples,
382 50% EtOH in 1/2 MS medium for mock samples, and only 1/2 MS medium for untreated
383 samples were transferred to a 96-well plate, and stored at −20°C until use. A single sterilized
384 seed was sown in each well of 96-well plates and grown in 50 μL of liquid 1/2 MS medium.
385 After 3 days of treatment at 4°C in the dark, the plants were cultivated at 20 °C for 5 days under
386 continuous light. SA/JA treatments were performed by adding 2 μL of 50× SA/JA mixed stock
387 solutions and 48 μL of liquid 1/2 MS medium to each well containing 5-day-old seedlings. This
388 allowed the 5-day-old seedlings to be incubated for 6 h under 64 variations of SA and JA
389 concentration conditions (Fig. 1A). To monitor the broad spectrum of early defense responses,
390 we treated with SA/JA for 6 h ((Hou et al., 2024; McGrath et al., 2005)). Mock and untreated
391 samples were treated for same time as above using 1% ethanol in 1/2 MS medium and only 1/2
392 MS medium, respectively. Four replicates of the plant were treated by each SA & JA condition,
393 respectively. We removed the medium and added 100 μL of direct-RT buffer (Kashima et al.,
394 2022) and a zirconia bead (YTZ-4, AS-ONE, Japan) to each well. Samples were ground using
395 the TissueLyser II (QIAGEN, MD, USA) by 2 rounds for 1.5 minutes of 2.5 Hz. The

396 homogenates were centrifuged at 3000 rpm for 10 min, and 50 μL of the supernatants were
397 stored as lysates at -20 °C. For test data of the transcriptomic biomarkers of SA/JA response
398 state, we performed the same procedure using Col-0, *npr3-1npr4-3* and *npr3-1npr4-3* under
399 twenty-five SA & JA concentration conditions made by combining five concentrations: 0 mM,
400 0.001 mM, 0.01 mM, 0.1 mM and 1 mM (Supplementary Fig. S6).
401
402 *RNA-Seq experiment and basic data analysis*
403 The 5 μL of lysate was used by RNA-Seq library preparation with the Lasy-seq v1.1
404 method (Kamitani et al., 2019). The library was sequenced by HiSeqX (Illumina, San Diego,
405 CA) with the paired-end 150+150bp mode. Trimomatic v0.3.3 (Bolger et al., 2014) was used
406 for trimming read data, and bowtie v1.1.2 (Langmead and Salzberg, 2012) and RSEM v1.3.0
407 (Li and Dewey, 2011)were used for expression quantification. For the following analysis, we
408 used log2(rpm+1) values calculated by the same procedure of the previous study (Kamitani et
409 al., 2019). The expression topography of all SA/JA responsive genes is shown in
410 Supplementary Figure S9.
411 We excluded samples with fewer than $10^{5.5}$ total reads from the analysis
412 (Supplementary Fig. S1A, B). We defined genes with more than 1.5 average $\log_2$ (RPM+1) as
413 the expressed genes (Supplementary Fig. S1A, C). We calculated the standard deviation (SD)
414 of the SA/JA-treated and control samples using the following procedure. To eliminate the effect
415 of differences in sample numbers, 63 samples were randomly selected from each of the SA/JA-
416 added samples and control samples. We calculated standard deviations among the 63 SA/JA-
417 added samples as $SD_{treated}$ and standard deviations among the 63 control samples as $SD_{control}$. In
418 the expressed genes, SA/JA responsive genes (3,001 genes in 370 samples) were selected based
419 on the ratio of the $SD_{treated}$ to $SD_{control}$ (Supplementary Fig. S1D).
420 We detected differentially expressed genes between the control and each concentration
421 treatment using a likelihood ratio test of the edgeR package (Robinson et al., 2010). 0 mM SA

422 and 0 mM JA, mock and untreated conditions were used as control samples. Expression data
423 were normalized by TMM (Robinson and Oshlack, 2010). The FDR was controlled using
424 Benjamini and Hochberg's method (Benjamini and Hochberg, 1995).
425
426 *Expression Topography*
427 The average expression levels were calculated for each condition. The average
428 expression levels of 8 × 8 conditions data for each gene were designated as an expression
429 topography. Smoothing by a 3 × 3 moving average filter was applied to the expression
430 topography. Z-scores of the smoothed expression data were calculated using the scale function
431 of R. Using the apcluster v.1.4.8 package (Bodenhofer et al., 2011), clustering was performed
432 by the affinity propagation method based on Z-scores of the smoothed expression
433 data. Pearson's correlation coefficient (r) was calculated using the Z-scores averaged over each
434 cluster of affinity propagation. Groups of clusters were determined by hierarchical clustering.
435 The correlation coefficients were as the distance between clusters, and the optimal number of
436 groups was estimated by the gap statistic (Fig. 2C). Gene Ontology annotations were obtained
437 from The Arabidopsis Information Resource (TAIR) on June 29, 2021. Fisher's exact test was
438 used to test the enrichment of GO terms. The multiple testing correction was performed with a
439 FDR. For these analyses, R 3.6.0 and 4.2.0 were used (R Core Team, 2024).
440
441 *Transcriptomic biomarker of SA/JA response state*
442 To create transcriptomic biomarkers correlated specifically with SA or JA, we
443 employed the method using ensemble learning and L1-regularized linear regression (Fukuda et
444 al., 2018) (Fig. 5A). Expression data of the 12,963 expressed genes from 370 samples in 64
445 concentration conditions were used as training data. The 1,296 genes, 10% of the expressed
446 genes, were randomly selected and used as input variables for LASSO (Tibshirani, 1996). The
447 hyperparameter λ of LASSO was determined by cross-validation. The selection of subset of

genes and LASSO were repeated 1,000 times. The median of the predicted values of the 1,000 regression models was used as the transcriptomic biomarker. Gene selection frequency was defined as the proportion of trials in which the gene had non-zero coefficient out of trials in which the gene was used as input variable (Supplementary Fig. S7). The test data of regression models were transcriptome data at 25 conditions of SA and JA combining 5 concentrations: 0, 0.001, 0.01, 0.1, and 1 mM. Analyses were performed using the glmnet package of R (R Core Team, 2024).

COMPETING INTERESTS

The authors declare that they have no competing interests.

FUNDING

This work was supported by JST CREST JPMJCR15O2, JST FOREST JPMJFR210B, JSPS (JP20H00423, JP23H00386, JP23K18156) and MEXT (JP23H04967) for AJN.

AUTHOR'S CONTRIBUTIONS

AJN and SB conceived the study. YN, YK and MK developed the assay system. AT and NMM conducted the RNA-Seq experiments. AT, TM and AJN analyzed the data. AT, and AJN wrote the manuscript with input from all co-authors.

ACKNOWLEDGEMENTS

We thank Dynacom Co., Ltd. (Chiba, Japan) for technical assistance with the analysis of RNA-Seq data.

DISCLOSURES

Conflicts of interest: No conflicts of interest declared.

DATA AVAILABLITY

The RNA-Seq data were submitted to the NCBI Sequence Read Archive repository under the BioProject PRJNA1232845. R scripts and data used in the analysis (count data, etc.) are available via the Figshare repository (https://doi.org/10.6084/m9.figshare.29163845.v1).

481

482 **REFERENCES**

483 Abuyusuf, M., Rubel, M.H., Kim, H.T., Jung, H.J., Nou, I.S., Park, J.I., 2023. Glucosinolates
484 and Biotic Stress Tolerance in Brassicaceae with Emphasis on Cabbage: A Review.
485 *Biochem Genet*, 61, 451–470. https://doi.org/10.1007/S10528-022-10269-6

486 Aires, A., Mota, V.R., Saavedra, M.J., Monteiro, A.A., Simões, M., Rosa, E.A.S., Bennett, R.N.,
487 2009. Initial in vitro evaluations of the antibacterial activities of glucosinolate enzymatic
488 hydrolysis products against plant pathogenic bacteria. *J Appl Microbiol*, 106, 2096–2105.
489 https://doi.org/10.1111/J.1365-2672.2009.04181.X

490 Aubert, Y., Widemann, E., Miesch, L., Pinot, F., Heitz, T., 2015. CYP94-mediated jasmonoyl-
491 isoleucine hormone oxidation shapes jasmonate profiles and attenuates defence responses
492 to Botrytis cinerea infection. *J Exp Bot*, 66, 3879–3892.
493 https://doi.org/10.1093/JXB/ERV190

494 Basit, F., Liu, J., An, J., Chen, M., He, C., Zhu, X., Li, Z., Hu, J., Guan, Y., 2021.
495 Brassinosteroids as a multidimensional regulator of plant physiological and molecular
496 responses under various environmental stresses. *Environ Sci Pollut Res Int*, 28, 44768–
497 44779. https://doi.org/10.1007/S11356-021-15087-8

498 Benjamini, Y., & Hochberg, Y., 1995. Controlling the False Discovery Rate: A Practical and
499 Powerful Approach to Multiple Testing. *J R Stat Soc Series B Stat Methodol*. Series B
500 Methodological, 57(1), 289–300. https://doi.org/10.1111/j.2517-6161.1995.tb02031.x

501 Bjornson, M., Kajala, K., Zipfel, C., Ding, P., 2020. Low-cost and High-throughput RNA-seq
502 Library Preparation for Illumina Sequencing from Plant Tissue. *Bio Protoc*, 10.
503 https://doi.org/10.21769/BIOPROTOC.3799

504 Bodenhofer, U., Kothmeier, A., Hochreiter, S., 2011. APCluster: an R package for affinity
505 propagation clustering. *Bioinformatics*, 27, 2463–2464.
506 https://doi.org/10.1093/bioinformatics/btr406

507 Bolger, A.M., Lohse, M., Usadel, B., 2014. Trimmomatic: a flexible trimmer for Illumina
508 sequence data. *Bioinformatics*, 30, 2114–2120.
509 https://doi.org/10.1093/BIOINFORMATICS/BTU170

510 Chauvin, A., Lenglet, A., Wolfender, J.L., Farmer, E.E., 2016. Paired Hierarchical Organization
511 of 13-Lipoxygenases in Arabidopsis. *Plants*, 2016, Vol. 5, Page 16 5, 16.
512 https://doi.org/10.3390/PLANTS5020016

513 Ding, Y., Sun, T., Ao, K., Peng, Y., Zhang, Yaxi, Li, X., Zhang, Yuelin, 2018. Opposite Roles of
514 Salicylic Acid Receptors NPR1 and NPR3/NPR4 in Transcriptional Regulation of Plant
515 Immunity. *Cell*, 173, 1454-1467.e10. https://doi.org/10.1016/j.cell.2018.03.044

516 Dodds, P.N., Rathjen, J.P., 2010. Plant immunity: towards an integrated view of plant–pathogen
517 interactions. *Nature Reviews Genetics*, 2010 11:8 11, 539–548.
518 https://doi.org/10.1038/nrg2812

519 Fernández-Calvo, P., Chini, A., Fernández-Barbero, G., Chico, J.-M., Gimenez-Ibanez, S.,
520 Geerinck, J., Eeckhout, D., Schweizer, F., Godoy, M., Franco-Zorrilla, J.M., Pauwels, L.,
521 Witters, E., Puga, M.I., Paz-Ares, J., Goossens, A., Reymond, P., De Jaeger, G., Solano,
522 R., 2011. The Arabidopsis bHLH Transcription Factors MYC3 and MYC4 Are Targets of
523 JAZ Repressors and Act Additively with MYC2 in the Activation of Jasmonate Responses.
524 *Plant Cell*, 23, 701–715. https://doi.org/10.1105/TPC.110.080788

525 Fritz, V.A., Justen, V.L., Bode, A.M., Schuster, T., Wang, M., 2010. Glucosinolate enhancement

526 in cabbage induced by jasmonic acid application. *HortScience*, 45, 1188–1191.
527 https://doi.org/10.21273/HORTSCI.45.8.1188

528 Fu, Z.Q., Yan, S., Saleh, A., Wang, W., Ruble, J., Oka, N., Mohan, R., Spoel, S.H., Tada, Y.,
529 Zheng, N., Dong, X., 2012. NPR3 and NPR4 are receptors for the immune signal salicylic
530 acid in plants. *Nature*, 486, 228–232. https://doi.org/10.1038/nature11162

531 Fukuda, A., Hirose, T., Aoki, N., Kondo, S., Yonekura, M., Kataoka, T., Ohto, C., Nagano, A.J.,
532 2018. Selection of transcripts affecting initial growth rate of rice backcrossed inbred lines
533 using RNA sequencing data. *Front Plant Sci*, 871, 414795.
534 https://doi.org/10.3389/FPLS.2018.01880

535 Ghorbel, M., Brini, F., Sharma, A., Landi, M., 2021. Role of jasmonic acid in plants: the
536 molecular point of view. *Plant Cell Reports*, 2021 40:8 40, 1471–1494.
537 https://doi.org/10.1007/S00299-021-02687-4

538 Glauser, G., Dubugnon, L., Mousavi, S.A.R., Rudaz, S., Wolfender, J.L., Farmer, E.E., 2009.
539 Velocity estimates for signal propagation leading to systemic jasmonic acid accumulation
540 in wounded Arabidopsis. *Journal of Biological Chemistry*, 284, 34506–34513.
541 https://doi.org/10.1074/jbc.M109.061432

542 Grode, A., Chen, S., Walker, E.D., Szendrei, Z., 2017. Onion Thrips (Thysanoptera: Thripidae)
543 Feeding Promotes Infection By Pantoea ananatis in Onion. *J Econ Entomol*, 110, 2301–
544 2307. https://doi.org/10.1093/JEE/TOX273

545 Guo, R., Shen, W., Qian, H., Zhang, M., Liu, L., Wang, Q., 2013. Jasmonic acid and glucose
546 synergistically modulate the accumulation of glucosinolates in Arabidopsis thaliana. *J Exp*
547 *Bot*, 64, 5707–5719. https://doi.org/10.1093/JXB/ERT348

548 Gupta S, Kaur R, Upadhyay A, Chauhan A, Tripathi V., 2024. Unveiling the secrets of abiotic
549 stress tolerance in plants through molecular and hormonal insights. *3 Biotech*. (10):252.
550 https://doi.org/10.1007/s13205-024-04083-7

551 Hashida, Y., Kyogoku, D., Tanaka, S.E., Mori, N., Tanabata, T., Watanabe, H., Nagano, A.J.,
552 2024. Field-crop transcriptome models are enhanced by measurements in systematically
553 controlled environments. *bioRxiv*, 2024.09.21.614268.
554 https://doi.org/10.1101/2024.09.21.614268

555 Hickman, R., Mendes, M.P., Verk, M.C. Van, Dijken, A.J.H. Van, Sora, J. Di, Denby, K.,
556 Pieterse, C.M.J., Wees, S.C.M. Van, 2019. Transcriptional Dynamics of the Salicylic Acid
557 Response and its Interplay with the Jasmonic Acid Pathway. *bioRxiv*, 742742.
558 https://doi.org/10.1101/742742

559 Hopkins, R.J., van Dam, N.M., van Loon, J.J.A., 2009. Role of Glucosinolates in Insect-Plant
560 Relationships and Multitrophic Interactions. *Annu Rev Entomol*, 54, 57-83.
561 https://doi.org/10.1146/annurev.ento.54.110807.090623

562 Hou, S., Tsuda, K., 2022. Salicylic acid and jasmonic acid crosstalk in plant immunity. *Essays*
563 *Biochem*, 66, 647–656. https://doi.org/10.1042/EBC20210090

564 Howe GA, Jander G., 2008. Plant immunity to insect herbivores. *Annu Rev Plant Biol*. 59:41-
565 66. https://doi.org/10.1146/annurev.arplant.59.032607.092825

566 Hwang, I.S., Hwang, B.K., 2010. Role of the pepper cytochrome P450 gene cacyp450a in
567 defense responses against microbial pathogens. *Planta*, 232, 1409–1421.
568 https://doi.org/10.1007/S00425-010-1266-Y

569 Jain, D., Khurana, J.P., 2018. Role of Pathogenesis-Related (PR) Proteins in Plant Defense

570 Mechanism. *Molecular Aspects of Plant-Pathogen Interaction*, 265–281.
571 https://doi.org/10.1007/978-981-10-7371-7_12

572 Javed, T., Wang, W., Yang, B., Shen, L., Sun, T., Gao, S.J., Zhang, S., 2025. Pathogenesis
573 related-1 proteins in plant defense: regulation and functional diversity. *Crit Rev Biotechnol*.
574 https://doi.org/10.1080/07388551.2024.2344583

575 Jeschke, V., Gershenzon, J., Vassão, D.G., 2016. A mode of action of glucosinolate-derived
576 isothiocyanates: Detoxification depletes glutathione and cysteine levels with ramifications
577 on protein metabolism in Spodoptera littoralis. *Insect Biochem Mol Biol*, 71, 37–48.
578 https://doi.org/10.1016/J.IBMB.2016.02.002

579 Kamitani, M., Kashima, M., Tezuka, A., Nagano, A.J., 2019. Lasy-Seq: a high-throughput
580 library preparation method for RNA-Seq and its application in the analysis of plant
581 responses to fluctuating temperatures. *Sci Rep*, 9, 1–14. https://doi.org/10.1038/s41598-
582 019-43600-0

583 Kashima, M., Kamitani, M., Nomura, Y., Hirata, H., Nagano, A.J., 2020. DeLTa-Seq: direct-
584 lysate targeted RNA-Seq from crude tissue lysate. *bioRxiv*, 2020.09.15.299180.
585 https://doi.org/10.1101/2020.09.15.299180

586 Kashima, M., Kamitani, M., Nomura, Y., Mori-Moriyama, N., Betsuyaku, S., Hirata, H.,
587 Nagano, A.J., 2022. DeLTa-Seq: direct-lysate targeted RNA-Seq from crude tissue lysate.
588 *Plant Methods*, 18, 1–18. https://doi.org/10.1186/s13007-022-00930-x

589 Kashima, M., Sakamoto, R.L., Saito, H., Ohkubo, S., Tezuka, A., Deguchi, A., Hashida, Y.,
590 Kurita, Y., Iwayama, K., Adachi, S., Nagano, A.J., 2021. Genomic Basis of Transcriptome
591 Dynamics in Rice under Field Conditions. *Plant Cell Physiol*.
592 https://doi.org/10.1093/PCP/PCAB088

593 Kenton, P., Mur, L.A.J., Atzorn, R., Wasternack, C., Draper, J., 1999. (-)-Jasmonic acid
594 accumulation in tobacco hypersensitive response lesions. *Molecular Plant-Microbe*
595 *Interactions*, 12, 74–78. https://doi.org/10.1094/MPMI.1999.12.1.74

596 Kitaoka, N., Kawaide, H., Amano, N., Matsubara, T., Nabeta, K., Takahashi, K., Matsuura, H.,
597 2014. CYP94B3 activity against jasmonic acid amino acid conjugates and the elucidation
598 of 12-O-β-glucopyranosyl-jasmonoyl-l-isoleucine as an additional metabolite.
599 *Phytochemistry*, 99, 6–13. https://doi.org/10.1016/J.PHYTOCHEM.2013.12.019

600 Kojima, M., Sakakibara, H., 2012. Highly sensitive high-throughput profiling of six
601 phytohormones using MS-probe modification and liquid chromatography-tandem mass
602 spectrometry. *Methods Mol Biol*, 918, 151–164. https://doi.org/10.1007/978-1-61779-995-
603 2_11

604 Koo, A.J.K., Cooke, T.F., Howe, G.A., 2011. Cytochrome P450 CYP94B3 mediates catabolism
605 and inactivation of the plant hormone jasmonoyl-L-isoleucine. *Proc Natl Acad Sci U S A*,
606 108, 9298–9303. https://doi.org/10.1073/pnas.1103542108

607 Langmead, B., Salzberg, S.L., 2012. Fast gapped-read alignment with Bowtie 2. *Nature*
608 *Methods*, 2012 9:4 9, 357–359. https://doi.org/10.1038/nmeth.1923

609 Li, B., Dewey, C.N., 2011. RSEM: accurate transcript quantification from RNA-Seq data with
610 or without a reference genome. *BMC Bioinformatics*, 2011 12:1 12, 1–16.
611 https://doi.org/10.1186/1471-2105-12-323

612 Li, N., Han, X., Feng, D., Yuan, D., Huang, L.J., 2019. Signaling Crosstalk between Salicylic
613 Acid and Ethylene/Jasmonate in Plant Defense: Do We Understand What They Are
614 Whispering?. *International Journal of Molecular Sciences*. 2019, Vol. 20, Page 671 20,
615 671. https://doi.org/10.3390/IJMS20030671

616 Liu, L., Sonbol, F.M., Huot, B., Gu, Y., Withers, J., Mwimba, M., Yao, J., He, S.Y., Dong, X.,
617 2016. Salicylic acid receptors activate jasmonic acid signalling through a non-canonical
618 pathway to promote effector-triggered immunity. *Nat Commun*, 7, 1–10.
619 https://doi.org/10.1038/ncomms13099

620 Madloo, P., Lema, M., Cartea, M.E., Soengas, P., 2021. Sclerotinia sclerotiorum Response to
621 Long Exposure to Glucosinolate Hydrolysis Products by Transcriptomic Approach.
622 *Microbiol Spectr*, 9. https://doi.org/10.1128/spectrum.00180-21

623 Maruri-López, I., Aviles-Baltazar, N.Y., Buchala, A., Serrano, M., 2019. Intra and Extracellular
624 Journey of the Phytohormone Salicylic Acid. *Front Plant Sci*, 0, 423.
625 https://doi.org/10.3389/FPLS.2019.00423

626 Mishina, T.E., Zeier, J., 2007. Pathogen-associated molecular pattern recognition rather than
627 development of tissue necrosis contributes to bacterial induction of systemic acquired
628 resistance in Arabidopsis. *Plant Journal*, 50, 500–513. https://doi.org/10.1111/J.1365-
629 313X.2007.03067.X

630 Munné-Bosch, S., Müller, M., 2013. Hormonal cross-talk in plant development and stress
631 responses. *Front Plant Sci*, 4, 76598. https://doi.org/10.3389/FPLS.2013.00529

632 Mur, L.A.J., Kenton, P., Atzorn, R., Miersch, O., Wasternack, C., 2006. The Outcomes of
633 Concentration-Specific Interactions between Salicylate and Jasmonate Signaling Include
634 Synergy, Antagonism, and Oxidative Stress Leading to Cell Death. *Plant Physiol*, 140,
635 249–262. https://doi.org/10.1104/PP.105.072348

636 Nagano, A.J., Kawagoe, T., Sugisaka, J., Honjo, M.N., Iwayama, K., Kudoh, H., 2019. Annual
637 transcriptome dynamics in natural environments reveals plant seasonal adaptation. *Nat*
638 *Plants*, 5, 74–83. https://doi.org/10.1038/s41477-018-0338-z

639 Nagano, A.J., Sato, Y., Mihara, M., Antonio, B.A., Motoyama, R., Itoh, H., Nagamura, Y., Izawa,
640 T., 2012. Deciphering and prediction of transcriptome dynamics under fluctuating field
641 conditions. *Cell*, 151, 1358–1369. https://doi.org/10.1016/j.cell.2012.10.048

642 Niu, D.-D., Liu, H.-X., Jiang, C.-H., Wang, Y.-P., Wang, Q.-Y., Jin, H.-L., Guo, J.-H., 2011. The
643 Plant Growth–Promoting Rhizobacterium Bacillus cereus AR156 Induces Systemic
644 Resistance in Arabidopsis thaliana by Simultaneously Activating Salicylate- and
645 Jasmonate/Ethylene-Dependent Signaling Pathways. *Molecular Plant-Microbe*
646 *Interactions*, 24, 533–542. https://doi.org/10.1094/mpmi-09-10-0213

647 Nobori, T., Monell, A., Lee, T.A., Sakata, Y., Shirahama, S., Zhou, J., Nery, J.R., Mine, A.,
648 Ecker, J.R., 2025. A rare PRIMER cell state in plant immunity. *Nature*.
649 https://doi.org/10.1038/s41586-024-08383-z

650 Ohnmeiss, T.E., McCloud, E.S., Lynds, G.Y., Baldwin, I.T., 1997. Within-plant relationships
651 among wounding, jasmonic acid, and nicotine implications for defence in Nicotiana
652 sylvestris. *New Phytol*, 137, 441–452. https://doi.org/10.1046/J.1469-8137.1997.00845.X

653 Pan, X., Wang, X., 2009. Profiling of plant hormones by mass spectrometry. *Journal of*
654 *Chromatography B*, 877, 2806–2813. https://doi.org/10.1016/J.JCHROMB.2009.04.024

655 Petřík, I., Hladík, P., Zhang, C., Pěnčík, A., Novák, O., 2024. Spatio-temporal plant
656 hormonomics: from tissue to subcellular resolution. *J Exp Bot*, 75.
657 https://doi.org/10.1093/JXB/ERAE267

658 Pieterse, C.M.J., Dicke, M., 2007. Plant interactions with microbes and insects: from molecular
659 mechanisms to ecology. *Trends Plant Sci*, 12, 564–569.
660 https://doi.org/10.1016/J.TPLANTS.2007.09.004

Pieterse, C.M.J., Ton, J., Van Loon, L.C., 2001. Cross-talk between plant defence signalling pathways: boost or burden? *AgBiotechNet 3*.

R Core Team, 2024. R: A Language and Environment for Statistical Computing. R Foundation for Statistical Computing, Vienna, Austria. https://www.R-project.org/.

Robert-Seilaniantz, A., Grant, M., Jones, J.D.G., 2011. Hormone crosstalk in plant disease and defense: More than just JASMONATE-SALICYLATE antagonism. *Annu Rev Phytopathol*, 49, 317–343. https://doi.org/10.1146/ANNUREV-PHYTO-073009-114447

Robinson, M.D., McCarthy, D.J., Smyth, G.K., 2010. edgeR: a Bioconductor package for differential expression analysis of digital gene expression data. *Bioinformatics*, 26, 139–140. https://doi.org/10.1093/BIOINFORMATICS/BTP616

Robinson, M.D., Oshlack, A., 2010. A scaling normalization method for differential expression analysis of RNA-seq data. *Genome Biol*, 11, 1–9. https://doi.org/10.1186/GB-2010-11-3-R25

Saito, R., Muto, T., Urano, H., Kitajima, T., Kato, N., Kwon, E., Ueda, M., 2023. (3R,7S) ‐ 12 ‐ Hydroxy ‐ jasmonoyl ‐ <scp>l</scp> ‐ isoleucine is the genuine bioactive stereoisomer of a jasmonate metabolite in Arabidopsis thaliana. *The Plant Journal*, 115, 709–723. https://doi.org/10.1111/tpj.16256

Santacruz, D., Enane, F.O., Fundel-Clemens, K., Giner, M., Wolf, G., Onstein, S., Klimek, C., Smith, Z., Wijayawardena, B., Viollet, C., 2022. Automation of high-throughput mRNA-seq library preparation: a robust, hands-free and time efficient methodology. *SLAS Discov*, 27, 140–147. https://doi.org/10.1016/j.slasd.2022.01.002

682 Savatin, D. V., Gramegna, G., Modesti, V., Cervone, F., 2014. Wounding in the plant tissue: The
683 defense of a dangerous passage. *Front Plant Sci*, 5, 111139.
684 https://doi.org/10.3389/fpls.2014.00470

685 Schweiger, R., Heise, A.M., Persicke, M., Müller, C., 2014. Interactions between the jasmonic
686 and salicylic acid pathway modulate the plant metabolome and affect herbivores of
687 different feeding types. *Plant Cell Environ*, 37, 1574–1585.
688 https://doi.org/10.1111/PCE.12257

689 Šimura, J., Antoniadi, I., Široká, J., Tarkowská, D., Strnad, M., Ljung, K., Novák, O., 2018.
690 Plant Hormonomics: Multiple Phytohormone Profiling by Targeted Metabolomics. *Plant*
691 *Physiol*, 177, 476–489. https://doi.org/10.1104/PP.18.00293

692 Spoel, S.H., Johnson, J.S., Dong, X., 2007. Regulation of tradeoffs between plant defenses
693 against pathogens with different lifestyles. *Proc Natl Acad Sci U S A*, 104, 18842–18847.
694 https://doi.org/10.1073/PNAS.0708139104

695 Spoel, S.H., Koornneef, A., Claessens, S.M.C., Korzelius, J.P., Van Pelt, J.A., Mueller, M.J.,
696 Buchala, A.J., Métraux, J.P., Brown, R., Kazan, K., Van Loon, L.C., Dong, X., Pieterse,
697 C.M.J., 2003. NPR1 modulates cross-talk between salicylate- and jasmonate-dependent
698 defense pathways through a novel function in the cytosol. *Plant Cell*, 15, 760–770.
699 https://doi.org/10.1105/TPC.009159

700 Takahashi, H., Kanayama, Y., Zheng, M.S., Kusano, T., Hase, S., Ikegami, M., Shah, J., 2004.
701 Antagonistic Interactions between the SA and JA Signaling Pathways in Arabidopsis
702 Modulate Expression of Defense Genes and Gene-for-Gene Resistance to Cucumber
703 Mosaic Virus. *Plant Cell Physiol*, 45, 803–809. https://doi.org/10.1093/PCP/PCH085

704 Thaler, J.S., Humphrey, P.T., Whiteman, N.K., 2012. Evolution of jasmonate and salicylate

705 signal crosstalk. *Trends Plant Sci*, 17, 260–270.
706 https://doi.org/10.1016/j.tplants.2012.02.010

707 Tibshirani, R., 1996. Regression Shrinkage and Selection Via the Lasso. *Journal of the Royal*
708 *Statistical Society*, Series B (Methodological) 58, 267–288.
709 https://doi.org/10.1111/J.2517-6161.1996.TB02080.X

710 Tsuda, K., Sato, M., Stoddard, T., Glazebrook, J., Katagiri, F., 2009. Network properties of
711 robust immunity in plants. *PLoS Genet*, 5.
712 https://doi.org/10.1371/JOURNAL.PGEN.1000772

713 Van Wees, S.C.M., De Swart, E.A.M., Van Pelt, J.A., Van Loon, L.C., Pieterse, C.M.J., 2000.
714 Enhancement of induced disease resistance by simultaneous activation of salicylate- and
715 jasmonate-dependent defense pathways in *Arabidopsis thaliana*. *Proc Natl Acad Sci U S*
716 *A*, 97, 8711–8716. https://doi.org/10.1073/pnas.130425197

717 Vrobel, O., Tarkowski, P., 2023. Can plant hormonomics be built on simple analysis? A review.
718 *Plant Methods*, 19, 1–22. https://doi.org/10.1186/S13007-023-01090-2

719 Wasternack, C., Hause, B., 2013. Jasmonates: biosynthesis, perception, signal transduction and
720 action in plant stress response, growth and development. An update to the 2007 review in
721 Annals of Botany. *Ann Bot*, 111, 1021–1058. https://doi.org/10.1093/AOB/MCT067

722 Weech, M.H., Chapleau, M., Pan, L., Ide, C., Bede, J.C., 2008. Caterpillar saliva interferes with
723 induced Arabidopsis thaliana defence responses via the systemic acquired resistance
724 pathway. *J Exp Bot*, 59, 2437–2448. https://doi.org/10.1093/JXB/ERN108

725 Wittstock, U., Burow, M., 2010. Glucosinolate Breakdown in Arabidopsis: Mechanism,
726 Regulation and Biological Significance. *Arabidopsis Book*, 8, e0134.

727 https://doi.org/10.1199/tab.0134

728 Yang, T.-H., Lenglet-Hilfiker, A., Stolz, S., Glauser, G., Farmer, E.E., 2020. Jasmonate
729 Precursor Biosynthetic Enzymes LOX3 and LOX4 Control Wound-Response Growth
730 Restriction. *Plant Physiol*, 184, 1172–1180. https://doi.org/10.1104/pp.20.00471

731 Zhang, N., Zhou, S., Yang, D., Fan, Z., 2020. Revealing Shared and Distinct Genes Responding
732 to JA and SA Signaling in Arabidopsis by Meta-Analysis. *Front Plant Sci*, 11, 512053.
733 https://doi.org/10.3389/FPLS.2020.00908

734 Zheng, X., Spivey, N.W., Zeng, W., Liu, P.-P., Fu, Z.Q., Klessig, D.F., He, S.Y., Dong, X., 2012.
735 Coronatine Promotes *Pseudomonas syringae* Virulence in Plants by Activating a Signaling
736 Cascade that Inhibits Salicylic Acid Accumulation. *Cell Host & Microbe*, 11, 587–596.
737 https://doi.org/10.1016/j.chom.2012.04.014

738 Hou, J., Ai, M., Li, J., Cui, X., Liu, Y., Yang, Q., 2024. Exogenous salicylic acid treatment
739 enhances the disease resistance of Panax vietnamensis by regulating secondary metabolite
740 production. Front Plant Sci 15. https://doi.org/10.3389/FPLS.2024.1428272

741 McGrath, K.C., Dombrecht, B., Manners, J.M., Schenk, P.M., Edgar, C.I., Maclean, D.J.,
742 Scheible, W.R., Udvardi, M.K., Kazan, K., 2005. Repressor- and Activator-Type Ethylene
743 Response Factors Functioning in Jasmonate Signaling and Disease Resistance Identified
744 via a Genome-Wide Screen of Arabidopsis Transcription Factor Gene Expression. Plant
745 Physiol 139, 949. https://doi.org/10.1104/PP.105.068544

746

747

748

749

750

751 **FIGURE LEGENDS**

752

753 **Figure1 Treatments of 64 combinations of SA/JA concentrations**

754 (A) SA/JA treatment for A. thaliana seedling using 96-well plates. Each sample was treated
755 with SA and JA at 64 conditions that were systematically combined among 8 concentrations: 0
756 mM, 0.001 mM, 0.0033 mM, 0.01 mM, 0.033 mM, 0.1 mM, 0.33 mM, and 1 mM. (B) A 96-
757 well plate with seedling just prior to the SA/JA treatment. (c - f) Expression topography of
758 genes related SA/JA responses. The horizontal axis of the heatmap corresponds to the
759 concentration of SA, and the vertical axis to the concentration of JA. The color of each cell
760 indicates the average log2(RPM + 1) for each concentration condition, n = 3~11. PR1 is a
761 marker gene for SA responses. (C). VSP1 is a marker gene for JA responses. (D). LOX3 is
762 encoding enzymes involved in JA synthesis (E). CYP94B3 is involved in the downregulation
763 of the JA response (F). (G - I) Principal component analysis of samples. Each point represents
764 samples. The color of each point indicates the log-transformed SA concentration (G), JA
765 concentration (H), and batch of the experiment (I).

766

767 **Figure 2 Forty-three clusters of expression topography represent various SA/JA**
768 **responses**

769 (A) Average expression topography of each cluster. The horizontal axis is the concentration of
770 SA, and the vertical axis is the concentration of JA. The colors represent the relative expression
771 values of the genes in each cluster, with lighter colors indicating higher expression levels. (B)
772 Upper 2 plots indicate concentration of SA/JA. Lower 2 plots show the relative expression
773 levels of the cluster A-02 and cluster C-01. Expression profiles of 40 genes in cluster A-02
774 and 64 genes in cluster C-01 are indicated as gray points and lines. Mean expression is indicated
775 as red lines. (C) Matrix of Pearson's correlation between the means of each cluster, sorted into
776 eight groups by hierarchical clustering.

Figure 3 Genes with similar expression topographies were involved in same biological prosses.

(A) GO enrichment in the clusters. The number of genes contained in each cluster is indicated in parentheses. The size of the circles indicates the number of genes. The color scale indicates the adjusted P-value (FDR) in the GO enrichment analysis. At the bottom of panel, The expression topographies of the clusters are shown. The colors represent the relative expression values of the genes in each cluster, with lighter colors indicating higher expression levels. A full list of enriched GO terms was indicated in Supplemental Table 2. (B, C) Relative expression levels of glucosinolate (GSL) synthesis genes. Mean expressions for 0 - 0.01 mM SA conditions (B) or 0.033 - 1 mM SA conditions (C) are plotted. The horizontal axis indicates JA concentration (mM), and the vertical axis indicates relative expression level. Aliphatic GSL synthesis genes are shown in red. Indole GSL synthesis genes are shown in blue. Bold lines indicate LOESS curves drawn for each glucosinolate type. (D-G) Expression topographies of aliphatic GSL synthesis genes. (H-K) Expression topographies of indole GSL synthesis genes. Data used in the panel (B) are indicated by green boxes.

Figure 4 Correlation between expression of single gene and SA/JA concentrations.

(A, B) Histogram of correlation coefficients between gene expression levels and SA concentrations (A), JA concentration (B). (C) Scatter plot of correlation coefficients between gene expression levels and SA/JA concentrations. Genes with the highest or lowest correlation coefficient are indicated as points. (D-G) Expression topographies of genes with the highest positive and negative correlation. HRG2 with the highest positive correlation coefficient for SA concentration (D), and UL4Z with the highest negative correlation (E). *AT2G47950* with the highest positive correlation coefficient for JA concentration (F), and SAUR6 with the highest negative correlation (G).

803

804 **Figure 5 Transcriptomic biomarker of SA/JA response state.** (A) Scheme of development
805 of a transcriptomic biomarker of SA/JA response state from RNA-seq data. See Materials and
806 Methods for further details. (B, C) Predictions of the transcriptomic biomarkers for training
807 data. Predicted value of the marker for SA response state and treated SA concentration (B).
808 Predicted value of the marker for JA response state and treated JA concentration (C). (D-G)
809 Predicted value of the transcriptomic biomarkers for test data of Col-0. Predicted value of the
810 SA marker and treated SA concentration for test data (D). Predicted value of the JA marker and
811 treated JA concentration for test data (E). Predicted value of the SA marker and treated JA
812 concentration for test data (F). Predicted value of the JA marker and treated SA concentration
813 for test data (G). The result of liner regression is shown in the blue line.

814

815 **Figure 6 SA/JA response states of *npr3/4* double mutants.** (A) Predictions of the JA marker
816 for *npr3/4* double mutants. Data obtained from 25 concentration conditions were grouped by
817 the treated SA concentrations. The vertical axis indicates the predicted SA concentrations by
818 the transcriptomic biomarker. (B) Liner regression between the treated SA concentrations and
819 the predicted SA concentrations. Formula for the liner regression was shown in the plot. (C)
820 Predictions of the JA marker for *npr3/4* double mutants. Data obtained from 25 concentration
821 conditions were grouped by the treated JA concentrations. The vertical axis indicates the
822 predicted JA concentrations by the transcriptomic biomarker. (D) Liner regression between the
823 treated JA concentrations and the predicted JA concentrations. Formula for the liner regression
824 was shown in the plot. Results of Mann-Whitney's U test were indicated as *: $P < 0.05$, **: P
825 < 0.01, ***: $P < 0.001$ and NS: not significant.

826

827

828 **SUPPLEMENTARY MATERIAL**

829 **Supplementary figure S1 Sample and gene filtering of RNA-seq data**

830 (A) Schematic flow of sample and gene filtering. (B) Histogram of total read counts for samples.
831 (C) Histogram of average expression levels. Genes whose expressions were greater than 1.5
832 were defined as expressed genes. (D) Scatter plot of $SD_{treated}$ and $SD_{control}$. Genes whose ratio of
833 $SD_{treated}$ to $SD_{control}$ were greater than 1.2 were defined as SA/JA responsive genes. Red lines
834 indicate thresholds.

835

836 **Supplementary Figure S2 Gene expression under combined SA/JA treatment.**

837 (A-D) Scatter plot of gene expression levels under SA/JA treatment conditions (mM). Black
838 circles represent $\log_2$ (RPM + 1) expression values for each individual RNA-seq sample. Upper
839 panels of x-axis are SA concentration and JA fixed at the value indicated above each panel.
840 Lower panels of x-axis are JA concentration and SA fixed at the value indicated above each
841 panel. The orange line indicates LOESS curves, and the light-grey band shows the 95 %
842 confidence interval.

843

844 **Supplementary figure S3. Principal-component analysis of transcriptome samples.**

845 (A) Scores of PC1 (19.3 % variance) plotted against log-transformed SA concentrations. The
846 PC1 primarily captures SA dose-dependent effects. (B) Scores of PC2 (6.7 % variance) plotted
847 against log-transformed JA concentrations. The PC2 primarily captures JA dose-dependent
848 effects. (C–F) Pairwise combinations of the subsequent PCs (PC1–PC8) colored by 96-well
849 plate number (Plate 1, red; Plate 2, green; Plate 3, blue; Plate 4, purple). The overlap among
850 ellipses shows that the Top 8 PCs were not captured by plate-to-plate variation.

851

852 **Supplementary figure S4 Number of differentially expressed genes by SA/JA treatment**

853 The number of differentially expressed genes between the control group and other 63 SA/JA

854 treatment conditions (FDR = 0.05). (A) Number of genes that were up-regulated by SA/JA
855 treatments. (B) Number of genes that were down-regulated by SA/JA treatments. (C) Number
856 of genes that were differentially expressed by SA/JA treatments. (D) Difference between the
857 number of up-regulated genes and the number down-regulated by SA/JA treatments.
858
859 **Supplementary figure S5. Relative expression levels of GSL synthesis genes**
860 (A-H) Relative expression levels of GSL synthesis genes at SA concentrations for 0 mM (A),
861 0.001 mM (B), 0.0033 mM (C), 0.01 mM (D), 0.033 mM (E), 0.1 mM (F), 0.33 mM (G), 1 mM
862 (H). The horizontal axis indicates JA concentration (mM), and the vertical axis indicates relative
863 expression level. Aliphatic GSL synthesis genes are shown in red. Indole GSL synthesis genes
864 are shown in blue. Bold lines indicate LOESS curves drawn for each glucosinolate type.
865
866 **Supplementary figure S6 Summary of test data of transcriptomic biomarkers for SA/JA**
867 **response states** (a-c) Layouts of SA treatment (A), JA treatment (B), and genotype (C) for test
868 data. Seedlings were treated with SA and JA at 25 conditions that were made by systematically
869 combining 5 concentrations of SA and JA: 0 mM, 0.001 mM, 0.01 mM, 0.1 mM, and 1 mM.
870 (D-F) Principal component analysis of samples of test data. The color of each point indicates
871 the genotypes (D), log-transformed SA concentrations (E) and JA concentrations (F).
872
873 **Supplementary figure S7 Selection frequency of genes in the transcriptomic biomarker**
874 (A) Scatter plot of selection frequency in the SA marker and JA marker. (B, C) Histogram of
875 selection frequency in the SA marker (B) and JA marker (C).
876
877 **Supplementary figure S8 Gene expressions of root-specific genes were detectable.**
878 (A) The total RNA contents of seedlings, shoots and roots. Error bars represent the standard
879 deviation (n = 12). (B) Expression topographies of genes expressed specifically and highly in

880 roots (A Christ et al., 2013). The horizontal axis of the heatmap corresponds to the concentration
881 of SA, and the vertical axis to the concentration of JA. The color of each cel indicates the
882 average log2(RPM + 1) for each concentration condition, n = 3~11.
883
884
885
886

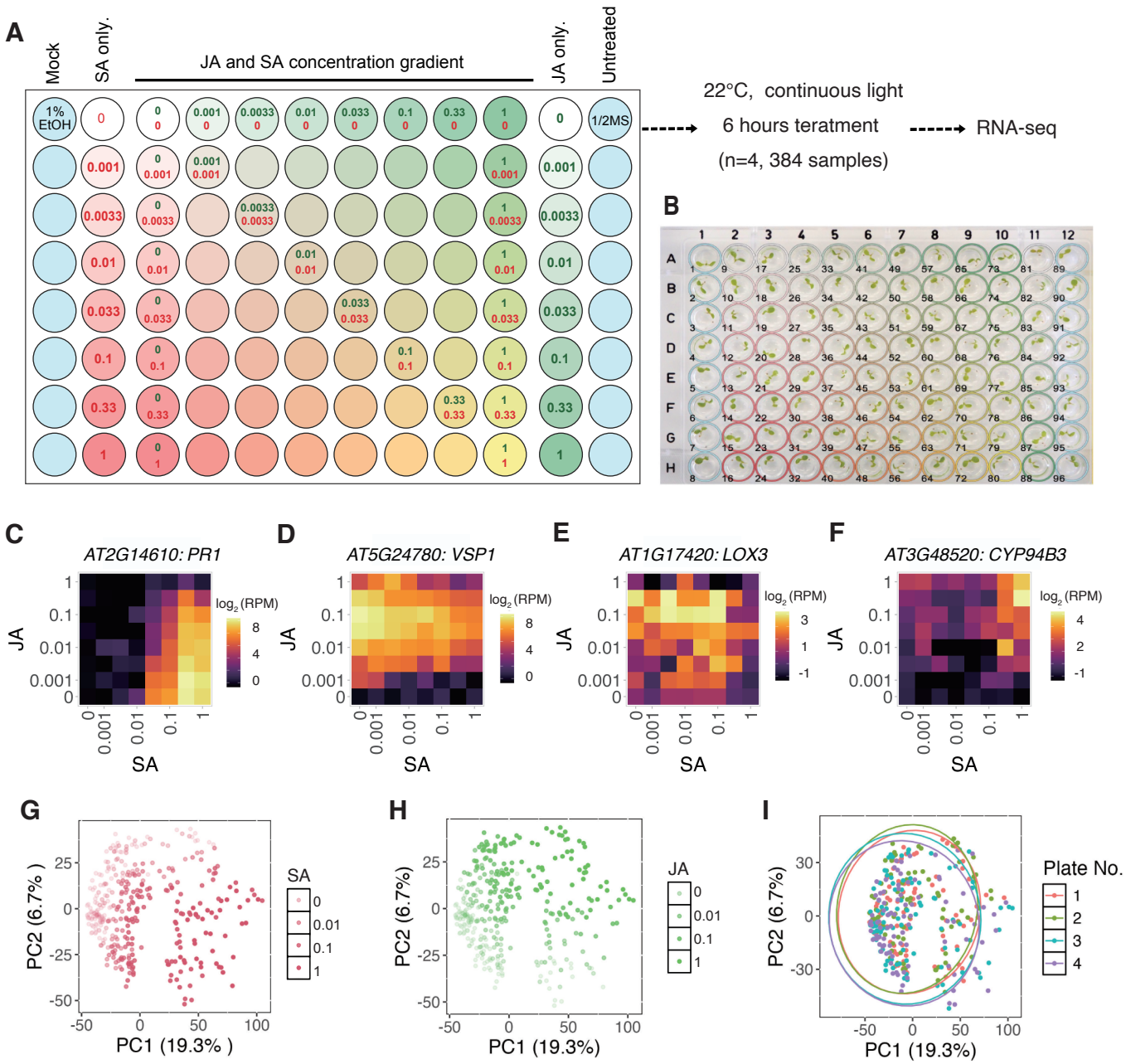

Figure1 Treatments of 64 combinations of SA/JA concentrations

(A) SA/JA treatment for *A. thaliana* seedling using 96-well plates. Each sample was treated with SA and JA at 64 conditions that were systematically combined among 8 concentrations: 0 mM, 0.001 mM, 0.0033 mM, 0.01 mM, 0.033 mM, 0.1 mM, 0.33 mM, and 1 mM. (B) A 96-well plate with seedling just prior to the SA/JA treatment. (C-F) Expression topography of genes related SA/JA responses. The horizontal axis of the heatmap corresponds to the concentration of SA, and the vertical axis to the concentration of JA. The color of each cell indicates the average log2(RPM + 1) for each concentration condition, n = 3~11. *PR1* is a marker gene for SA responses. (C). VSP1 is a marker gene for JA responses. (D). LOX3 is encoding enzymes involved in JA synthesis (E). CYP94B3 is involved in the downregulation of the JA response (F). (G - I) Principal component analysis of samples. Each point represents samples. The color of each point indicates the log-transformed SA concentration (G), JA concentration (H), and batch of the experiment (I).

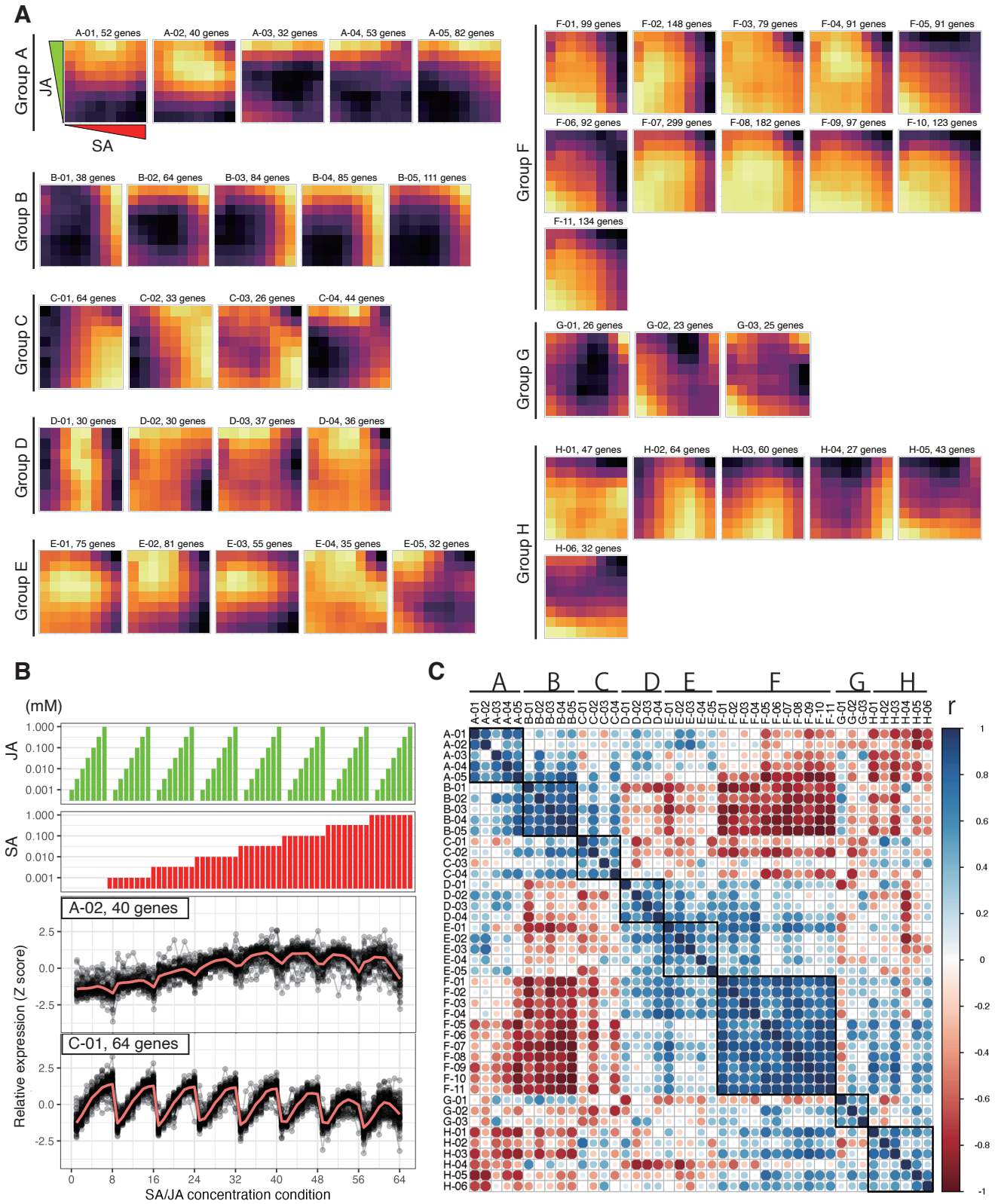

Figure 2 Forty-three AP clusters of expression topography represent various SA/JA responses

(A) Average expression topography of each cluster. The horizontal axis is the concentration of SA, and the vertical axis is the concentration of JA. The colors represent the relative expression values of the genes in each cluster, with lighter colors indicating higher expression levels. (B) Upper 2 plots indicate concentration of SA/JA. Lower 2 plots show the relative expression levels of the AP cluster A-02 and AP cluster C-01. Expression profiles of 40 genes in AP cluster A-02 and 64 genes in AP cluster C-01 are indicated as gray points and lines. Mean expression is indicated as red lines. (C) Matrix of Pearson's correlation between the means of each cluster, sorted into eight groups by hierarchical clustering.

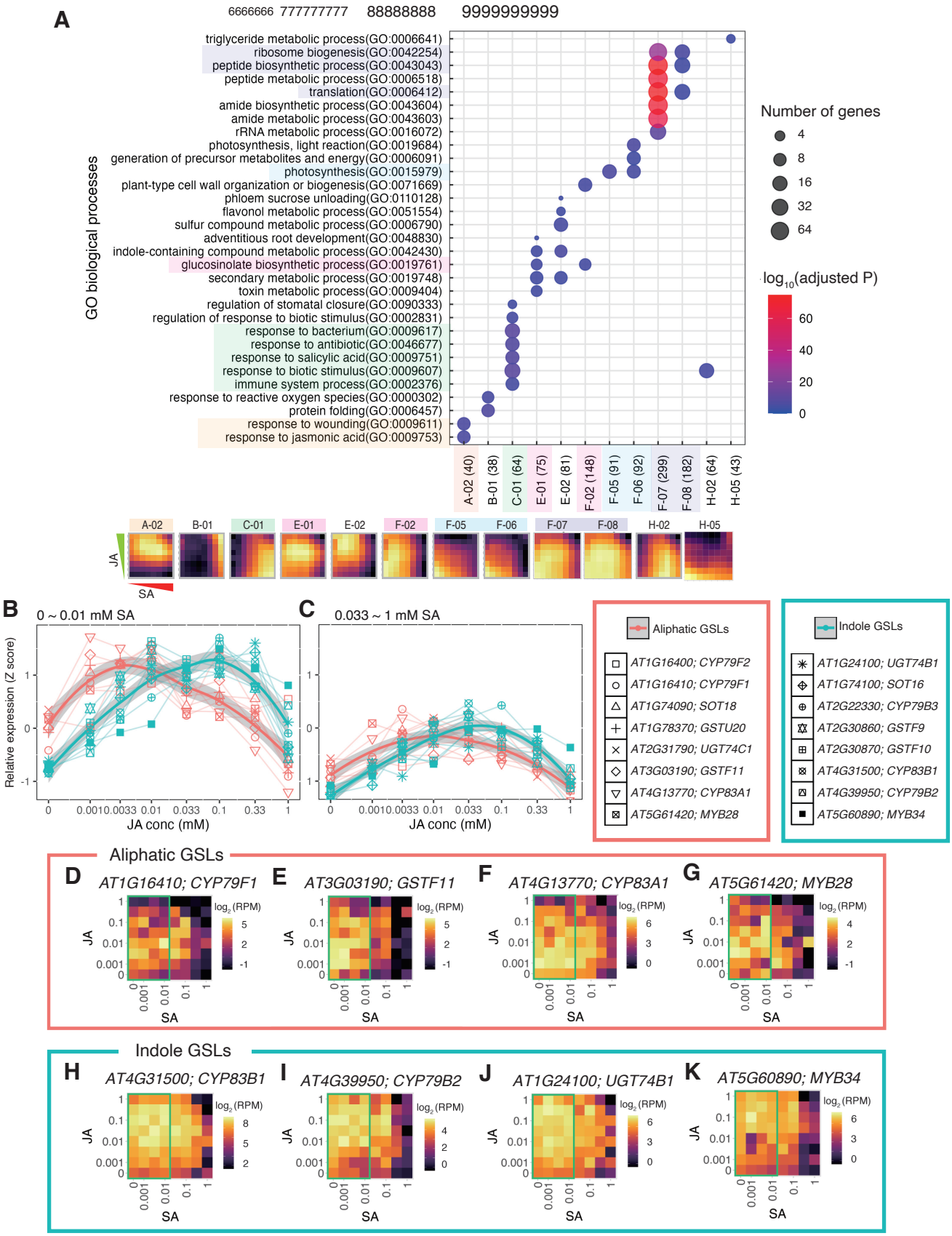

Figure 3 Genes with similar expression topographies were involved in same biological prosses.

(A) GO enrichment in the AP clusters. The number of genes contained in each cluster is indicated in parentheses. The size of the circles indicates the number of genes. The color scale indicates the adjusted P-value (FDR) in the GO enrichment analysis. The expression topographies of the AP clusters are shown. The colors represent the relative expression values of the genes in each cluster, with lighter colors indicating higher expression levels. A full list of enriched GO terms was indicated in Supplemental Table 1. (B, C) Relative expression levels of glucosinolate (GSL) synthesis genes. Mean expressions for 0 - 0.01 mM SA conditions (B) or 0.033 - 1 mM SA conditions (C) are plotted. The horizontal axis indicates JA concentration (mM), and the vertical axis indicates relative expression level. Aliphatic GSL synthesis genes are shown in red. Indole GSL synthesis genes are shown in blue. Bold lines indicate LOESS curves drawn for each glucosinolate type. (D-G) Expression topographies of aliphatic GSL synthesis genes; (D) AT1G16410, (E) AT3G03190, (F) AT4G13770 and (G) AT1G24100. (H-K) Expression topographies of indole GSL synthesis genes; (H) AT4G31500, (I) AT4G39950, (J) AT5G60890 and (K) AT5G61420. Data used in the panel (B) are indicated by green boxes.

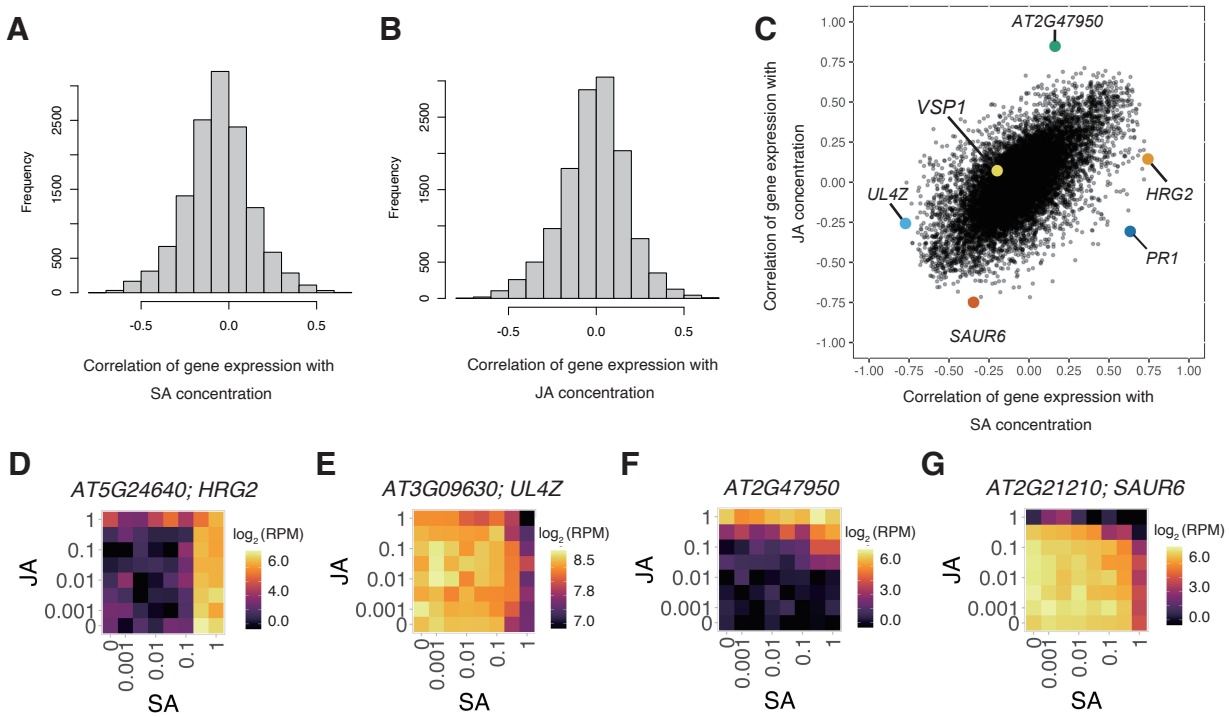

Figure 4 Correlation between expression of single gene and SA/JA concentrations.

(A, B) Histogram of correlation coefficients between gene expression levels and SA concentrations (A), JA concentration (B). (C) Scatter plot of correlation coefficients between gene expression levels and SA/JA concentrations. Genes with the highest or lowest correlation coefficient are indicated as points. (D-G) Expression topographies of genes with the highest positive and negative correlation. HRG2 with the highest positive correlation coefficient for SA concentration (D), and UL4Z with the highest negative correlation (E). AT2G47950 with the highest positive correlation coefficient for JA concentration (F), and SAUR6 with the highest negative correlation (G).

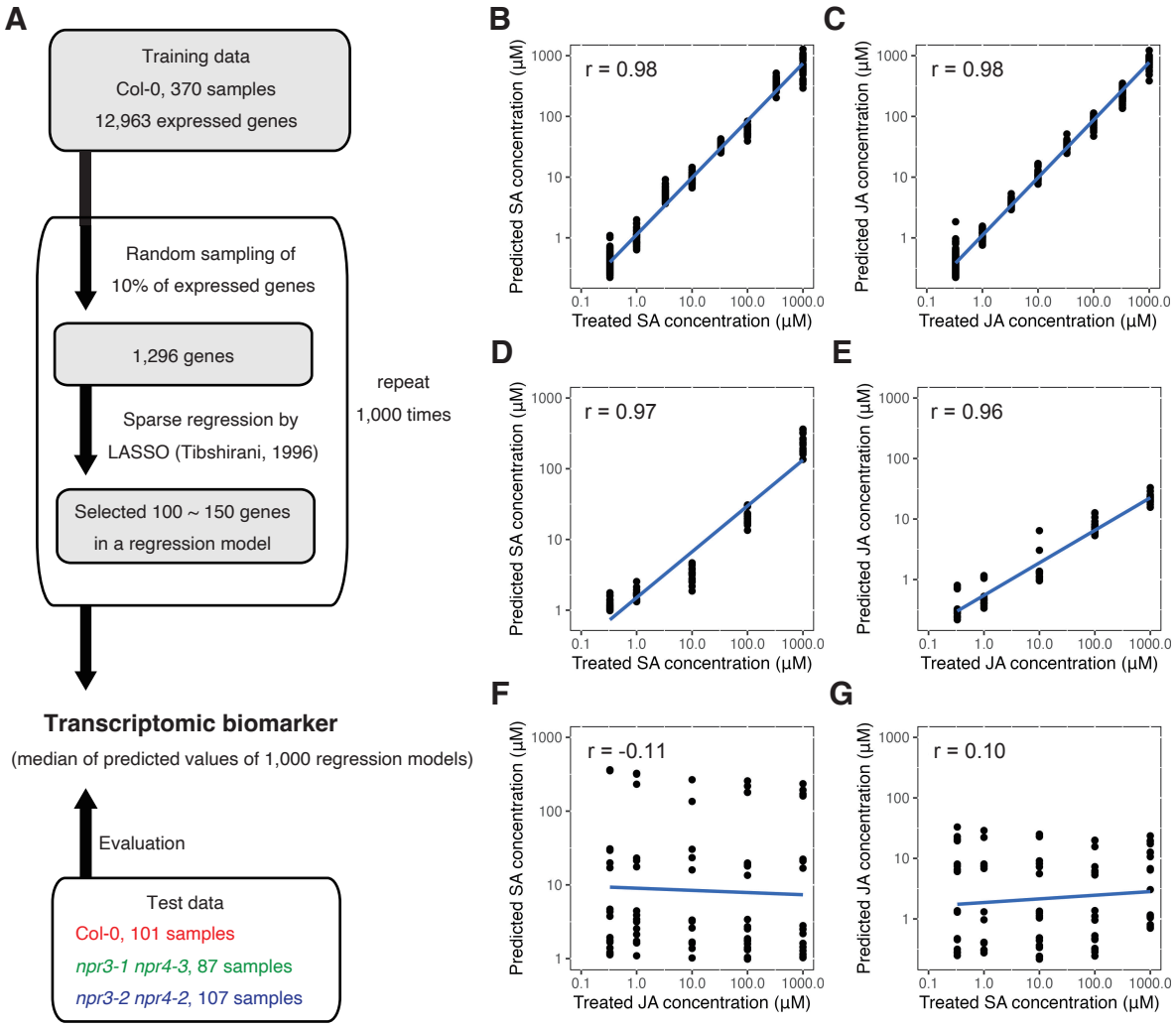

Figure 5 Transcriptomic biomarker of SA/JA response state.

(A) Scheme of development of a transcriptomic biomarker of SA/JA response state from RNA-seq data. See Materials and Methods for further details. (B, C) Predictions of the transcriptomic biomarkers for training data. Predicted value of the marker for SA response state and treated SA concentration (B). Predicted value of the marker for JA response state and treated JA concentration (C). (D-G) Predicted value of the transcriptomic biomarkers for test data of Col-0. Predicted value of the SA marker and treated SA concentration for test data (D). Predicted value of the JA marker and treated JA concentration for test data (E). Predicted value of the SA marker and treated JA concentration for test data (F). Predicted value of the JA marker and treated SA concentration for test data (G). The result of liner regression is shown in the blue line.

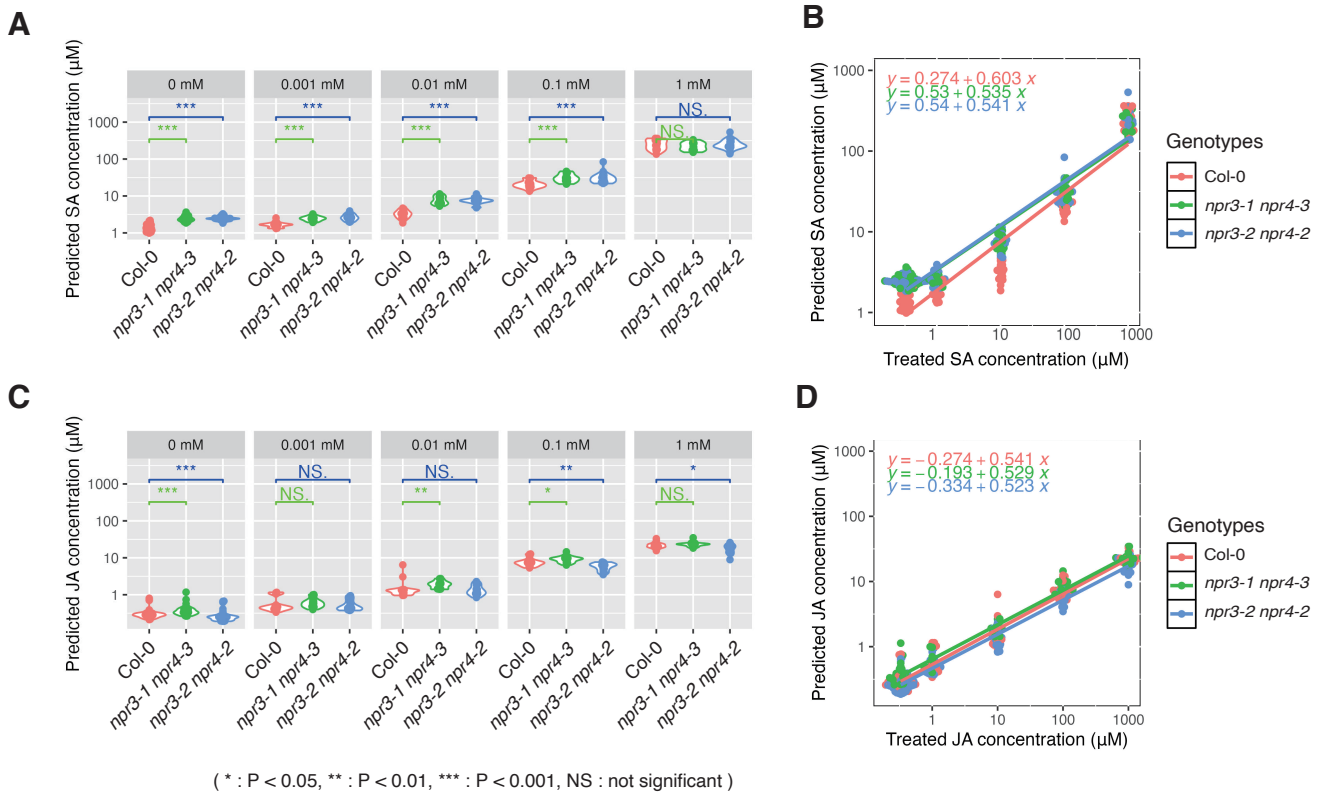

Figure 6 SA/JA response states of npr3/4 double mutants.

(A) Predictions of the JA marker for npr3/4 double mutants. Data obtained from 25 concentration conditions were grouped by the treated SA concentrations. The vertical axis indicates the predicted SA concentrations by the transcriptomic biomarker. (B) Liner regression between the treated SA concentrations and the predicted SA concentrations. Formula for the liner regression was shown in the plot. (C) Predictions of the JA marker for npr3/4 double mutants. Data obtained from 25 concentration conditions were grouped by the treated JA concentrations. The vertical axis indicates the predicted JA concentrations by the transcriptomic biomarker. (D) Liner regression between the treated JA concentrations and the predicted JA concentrations. Formula for the liner regression was shown in the plot. Results of Mann-Whitney's U test were indicated as *: $P < 0.05$, **: $P < 0.01$, ***: $P < 0.001$ and NS: not significant.